

The Catalytic Oxidation of 1-Butene over Bismuth Molybdate Catalysts

III. The Reduction of Bismuth Oxide, Molybdenum Oxide, Bismuth Molybdate, and of some Nonstoichiometric Molybdenum Oxides with 1-Butene

PH. A. BATIST, C. J. KAPTEIJNS, B. C. LIPPENS, AND G. C. A. SCHUIT

From the Department of Inorganic Chemistry, Technological University, Eindhoven, The Netherlands

Received May 11, 1966; revised August 1, 1966

The reaction of 1-butene with bismuth molybdate, MoO₃, and some nonstoichiometric Mo oxides was studied as a function of time and temperature at virtually constant hydrocarbon pressure. The reaction proceeds to four-valent molybdenum and to zero-valent bismuth. It is initially fast on bismuth molybdate, but MoO₃ and some of the nonstoichiometric oxides show an induction period. The hydrocarbon products of the reduction are butadiene, CO, and CO₂, while also isomerization of 1-butene to *cis*- and *trans*-2-butene is observed.

The kinetic analysis of the rate as a function of the time was made on the basis of a model proposed by Crank and extended by Haul, Just, and Dürnberg, consisting of a surface reaction followed by oxygen vacancy diffusion in the solid. The model furnishes quantitative values for a surface rate constant and a diffusion constant in the interior.

The surface reaction was observed to be fast enough to account for the rate of the oxidative dehydrogenation. Since also the nature of the reduction products is similar to that observed during the catalytic reaction it is concluded that the latter consists of a surface reduction followed by a reoxidation with gaseous oxygen.

The diffusion constants observed could be given as

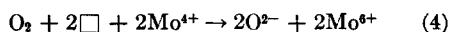
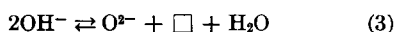
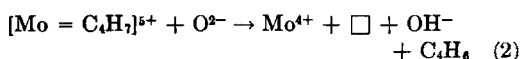
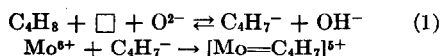
$$\log D = \log D_0 - E_D/RT$$

Bismuth molybdate	$\log D_0 = -3.73$	$E_D = 29.3 \text{ kcal mole}^{-1}$
MoO ₃	$\log D_0 = -5.62$	$E_D = 22.1 \text{ kcal mole}^{-1}$

The numerical values for D observed for the MoO₃ reduction are equal to those obtainable from the experiments of von Destinin-Forstmann for the reduction of MoO₃ by hydrogen.

INTRODUCTION

In a preceding paper (1) we formulated a mechanism for the catalytic oxidation of 1-butene to butadiene over MoO₃ and Bi₂O₃ + MoO₃ catalysts that can be summarized as follows:



Here, \square is an anion vacancy at the surface and $[\text{Mo}=\text{C}_4\text{H}_7]^{5+}$ is a π complex of Mo⁶⁺ and the allyl carbanion. The reduction of Mo⁶⁺ to Mo⁴⁺ is probably not the only type of cation reduction that may occur: the presence of Mo⁵⁺ or of some reduced form of Biⁿ⁺ is not excluded. The reverse of reaction (1) was supposed to lead to the formation of *cis*- and *trans*-2-butene. Furthermore it was postulated that the reoxidation of the reduced catalyst [reaction (4)] is fast and that the equilibrium for the hydroxylation-dehydroxylation reaction (3) is on the

left side for MoO_3 and on the right side for $\text{Bi}_2\text{O}_3\text{—MoO}_3$.

The presence of the intermediate allyl complex of vital importance for the relevancy of this reaction mechanism was proved earlier by Adams (2) on the one hand and by Sachtler and de Boer (3) on the other hand. One of its essential characteristics, however, the successive reduction and oxidation of the catalyst so far remains unproved. For this assumption to be applicable one should demand that reduction of the catalyst by 1-butene should (a) proceed at a rate comparable to that of the oxidative dehydrogenation reaction; (b) lead to products similar to those observed there. Strictly speaking, this only applies for the initial stages of the reduction since later on the partially reduced catalyst might differ in its characteristics as to rate and selectivity from the fully oxidized sample.

This paper reports on the results obtained by reduction of MoO_3 -containing catalysts by 1-butene and contains a proof for the correctness of the reduction-oxidation model given above. Since reduction of MoO_3 might proceed via the formation of nonstoichiometric Mo oxides, some of these were prepared and also investigated as to their reduction properties. Moreover, an abnormal, i.e., less active, Bi/Mo catalyst (Bi/Mo catalyst (B-50/50) was put to the same test.

Reduction of the oxide entails a depletion of oxygen in the interior of the solid and therefore the cooperation of diffusional processes. In order to interpret the reduction correctly, especially in the initial stages, an appropriate model to treat the combined influence of surface reduction and oxygen diffusion should be available.

THE MATHEMATICAL MODEL FOR A SURFACE REACTION FOLLOWED BY DIFFUSION IN THE INTERIOR OF THE SOLID

Species that are removed from the solid are the oxygen ions that are converted to water in the gaseous phase. Alternatively one might say that anion vacancies are added to the solid, the hydrocarbon being the source of these vacancies. However,

oxygen ion diffusion and vacancy diffusion are identical except for the sign.

In the solid Fick's law demands that

$$\partial C/\partial t = D(\partial^2 C/\partial x^2) \quad (1)$$

where C is the concentration of the migrating species be it oxygen or vacancy. If it is assumed that diffusion occurs only in one direction the solid therefore can be considered as being semiinfinite with one boundary plane surface. To solve the differential equation, the initial and boundary conditions have to be stated. We choose now to define these in accordance with Crank (4). See also Haul, Just, and Dumbgen (5), who applied a similar model.

The initial condition is given by assuming a concentration C_0 in the gas phase and C_s in the solid at $t = 0$. The concentration C_0 either representing 1-butene (= vacancies) or water (= oxygen ions) is not supposed to change during the reduction. The rate at which the diffusing species enters into the surface (vacancies) or leaves it (oxygen ions) should furnish the boundary condition and is supposed to be given by

$$K_s(C_0 - C_s) \quad (2)$$

where C_s is the concentration at the surface, and K_s , a constant with dimension sec^{-1} . This decrease or increase is counteracted by the diffusion from or to the interior, the rate of which is given by

$$-D|\partial C_s/\partial x| \quad \text{for} \quad x = 0$$

where D is the diffusion constant ($\text{cm}^2 \text{sec}^{-1}$).

Under stationary conditions C_s is supposed to change only slowly, hence

$$|\partial C_s/\partial t| = 0$$

To equate the two components of transport, it should be considered that D , the diffusion constant, consists of a jump frequency multiplied by the square of a jump distance λ , that is of the order of magnitude of the lattice constant. Hence

$$-D|\partial C/\partial x|_{x=0} = K_s\lambda(C_0 - C_s) \quad (3)$$

or

$$-D|\partial C/\partial x|_{x=0} = \alpha(C_0 - C_s) \quad (4)$$

with $\alpha = K_s \lambda$ and the dimension of α , cm sec^{-1} . Under these conditions the solution of the differential equation is

$$M_t = [(C_0 - C_s)/h] \{ \text{e.erfc} [h(Dt)^{1/2}] - 1 + (2/\pi^{1/2})h(Dt)^{1/2} \} \quad (5)$$

where $h = \alpha/D$; $\text{e.erfc } \varphi = e^{\varphi^2} (1 - \text{erf } \varphi)$; and M_t is the amount of material lost from the solid at time t per unit surface (g cm^{-2}). The total amount of material lost at time t is SgM_t , where S is the surface area (cm^2) and g is the weight of solid present. Now the total material that can be transported is $M_s = (C_0 - C_s)V$, where V is the volume of the material. Therefore $g(C_0 - C_s) = \rho M_s$, where ρ is the density of the solid. Moreover, the amount of material lost has served to dehydrogenate a certain amount of butene to butadiene.

If X is the butene fraction relative to the initial concentration in the gas phase at time t and X_s that at complete reduction of the solid sample, then Eq. (5) can be rewritten as

$$\frac{1 - X}{1 - X_s} = \frac{S\rho}{h} \left\{ \text{e.erfc} [h(Dt)^{1/2}] - 1 + \frac{2}{\pi^{1/2}} h(Dt)^{1/2} \right\} \quad (6)$$

The first term between brackets is equal to one at $t = 0$, and decreases later on to zero. As an approximation we can write

$$(1 - X)/(1 - X_s) = -A + Bt^{1/2} \quad (7)$$

in which $A = S\rho D/\alpha$ and $B = (2/\pi^{1/2})S\rho D^{1/2}$. Equation (7) is only applicable within a restricted range of conversions since at low conversion the e.erfc term cannot be neglected versus the remaining terms in the brackets, while at higher conversions the breakdown of our original assumption of a semiinfinite medium will make itself increasingly felt. In order to define these limits in an approximate manner we introduce two new dimensionless groups: $(t/t_0)^{1/2}$ and $S\rho D/\alpha$ where

$$t_0^{1/2} = D^{1/2}/\alpha$$

and rewrite Eq. (6) in a new form

$$\frac{1 - X}{1 - X_s} \frac{\alpha}{DS\rho} = \Sigma = \left\{ \text{e.erfc} \left(\frac{t}{t_0} \right)^{1/2} - 1 + \frac{2}{\sqrt{\pi}} \left(\frac{t}{t_0} \right)^{1/2} \right\} \quad (8)$$

Inspection reveals that the e.erfc term may only be neglected when $(t/t_0)^{1/2}$ surpasses the number 1.4. Moreover, since the maximal value of the left-hand side of Eq. (8) is equal to $\alpha/DS\rho$, the points for which the term within brackets exceed $0.9\alpha/DS\rho$ are to be neglected.

Haul *et al.* (6) made a theoretical study of the properties of the integrated equation in particular for those cases where t_0 is high, i.e., α is relatively small compared to D , so that most of the experimental points become located in that part of Eq. (8) where Eq. (7) is still poor as an approximation. They published tables for this region obtained by numerical computation with the help of which accurate fits for D and α are obtainable even for relatively unfavorable situations such as a low rate of the surface reaction.

Our results, to be discussed later on, shall be found to be divided in two categories. In one category t_0 is small so that there is no difficulty in fitting most of the data to a relation such as (7). Values for D and α obtained herefrom were then inserted in plots according to (8). Since the right-hand side of this equation is a single curve all experimental data should fit this curve including those obtained at relatively short times of reduction. It sometimes proved necessary to correct the original values of D and α in order to acquire a better fit but these corrections were small. The final choices of D and α are illustrated by showing the fit of the experimental data in plots according to (8). In another category, however, we found a peculiar behavior of the reaction kinetics not readily reconcilable with Eq. (6). One observes an initial period during which the reaction accelerates in what seems to be an exponential law. Plots of the results according to (7) show this relation to be a satisfactory approximation

with, however, relatively high values of t_0 . As could be expected in view of the exponential rise in the beginning of the reaction the data do not fit Eq. (8). We believe that this is caused by the fact that the boundary condition (2) is not applicable any more.

Starting from the reaction mechanism proposed above and assuming reaction (1) to be rate-determining, the rate law of the surface reaction should be written as

$$k'' p_c N_s \theta_s (1 - \theta_s) z \quad (9)$$

where k'' is the reaction constant, p_c the partial pressure of 1-butene (supposed to remain constant during the reaction), N_s the number of sites per cm^2 surface, z the number of nearest-neighbor sites to a certain site, θ_s the fractional coverage of the sites with O^{2-} and $(1 - \theta_s)$ the fractional coverage with anion vacancies. Clearly $N_s z \theta_s (1 - \theta_s)$ represents the number of pairs of sites constituted from an O^{2-} ion and a vacancy.

Now, if θ_0 (i.e., θ_s at $t = 0$) is low at the start of the reaction, Eq. (9) degenerates into Eq. (2) since $1 - \theta_s \simeq 1$, $N_s \theta_s \simeq C_s$ and C_0 can be taken to be zero. However, if $\theta_0 \simeq 1$, the surface reaction behaves differently: it starts by being slow to increase in speed later on. It appears as if the domain of validity of (8) is preceded by another one in which the surface reaction develops to its final form.

The integration of Fick's equation with (9) as the boundary condition has not, we believe, been attempted so far and at any rate appears to offer considerable difficulties. One can, however, try to ascertain what its consequences are for the initial stages of the reaction by an approximative treatment.

The situation at the surface can be represented by

$$-\frac{dN}{dt} = k' N_s \theta_s (1 - \theta_s) - \frac{D N_s}{\lambda} \left. \frac{\partial \theta}{\partial x} \right|_{x=0} \quad (10)$$

where $-dN/dt$ is the number of oxygen atoms lost from the surface per cm^2 and per unit time, $k' = k'' p_c z$, and θ is the fractional coverage of layers in the solid parallel to the surface layer by O^{2-} ions.

We shall now approximate the O^{2-} gradient in the solid by putting

$$\left. \frac{\partial \theta}{\partial x} \right|_{x=0} = (1 - \theta_s) / \delta \quad (11)$$

where δ is a certain length, indicative of the degree of reduction of the solid during the initial surface reduction. Hence

$$-\frac{d\theta_s}{dt} = k' \theta_s (1 - \theta_s) - \frac{D}{\lambda} \frac{(1 - \theta_s)}{\delta} \quad (12)$$

After integration

$$\theta_s = \frac{1 + \eta P e^{\varphi t}}{1 + P e^{\varphi t}} \quad (13)$$

where

$$\eta = D/k' \lambda \delta = D/\alpha \delta \quad \varphi = k'(1 - \eta)$$

Clearly θ_s starts by being equal to θ_0 at $t = 0$ to level out at η for $t = \infty$.

At the limit $d\theta_s/dt = 0$ and the stationary state required earlier is established. If θ_0 is near to one and η is considerably smaller than one, P is small. The total amount of material converted is

$$\frac{1}{2} \{ (1 - \theta_s) - (1 - \theta_0) \} \frac{\delta}{l} = \frac{1}{2} (\theta_0 - \theta_s) \frac{\delta}{l}$$

where l is the average length of the semi-infinite slabs

$$\frac{1 - X}{1 - X_e} = \frac{1}{2} \frac{P(1 - \eta)(e^{\varphi t} - 1)}{(1 + P)(1 + P e^{\varphi t})} \frac{\delta}{l} \quad (14)$$

For P small, this degenerates for the start of the reduction to

$$\frac{1 - X}{1 - X_e} = \frac{1}{2} P(1 - \eta) e^{\varphi t} \frac{\delta}{l}$$

which causes us to expect an initial rate that increases exponentially with time.

Since η is of the order of 1 and $S_p = 1/l$ an approximate impression of the depth of penetration of the reduction during the initial stages can be obtained from

$$\delta/l \simeq \rho S D / \alpha \quad (15)$$

Obviously, this method of dealing with the initial situation is indeed very approximate and its sole merit probably lies in pointing out that under certain circumstances (i.e.,

very few surface vacancies and a low rate of the surface reaction) the particular nature of this surface reaction may reveal itself in the kinetics of the reduction by introducing what is in effect an induction period.

EXPERIMENTAL PROCEDURE

Preparation of the oxides. Bi_2O_3 was prepared by heating of $\text{Bi}(\text{NO}_3)_3 \cdot 5\text{H}_2\text{O}$ p.a at 600°C during 20 hr. MoO_3 p.a, manufactured by Merck, was used as such without previous calcination except in one experiment in which it was precalcined at 600°C during 20 hr. The bismuth molybdates used were the catalysts B-48/52 and B-50/50. Their preparations and compositions have already been described in our previous paper (1). The nonstoichiometric compounds Mo_4O_{11} , $\text{Mo}_{17}\text{O}_{47}$, Mo_8O_{23} , and $\text{Mo}_{18}\text{O}_{52}$ were prepared from mixtures of MoO_3 and MoO_2 and use has been made of the heating method of Magnéli and Kihlberg (7). MoO_3 and MoO_2 were mixed in such a ratio that the compositions tallied with those of the compounds mentioned above. The mixtures were heated in vacuum in sealed tubes for hours after which they were cooled down rapidly in ice water in order to avoid side reactions. Table 1 shows the circumstances during the preparation.

TABLE 1
PREPARATION OF MOLYBDENUM OXIDES

Compound	Reaction time (hr)	Reaction temperature ($^\circ\text{C}$)	Color of the product
Mo_4O_{11}	4	700	Violet
$\text{Mo}_{17}\text{O}_{47}$	200	530	Grayish-blue
Mo_8O_{23}	50	660	Blue
$\text{Mo}_{18}\text{O}_{52}$	50	625	Blue

The two blue-colored compounds were of a metallic appearance. The compounds prepared were identified by comparing their X-ray diagrams with those given by Kihlberg. The interplanar spacings (d values) were found to agree with those reported by Magnéli and Kihlberg.

Circulation apparatus. The procedure followed was circulation of a mixture of helium and 1-butene over the oxide in the absence of air. 1-Butene was present in excess

as calculated with respect to maximal reduction of the oxide used. Normally we started with volumes of 1-butene varying from 46 to 49 cm^3 on 200 mg metal oxide, the 1-butene being diluted with helium to a mol ratio of He/1-butene equal to 4.5.

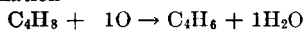
The essential parts of the apparatus were a microreactor of quartz, a sampling valve, a piston pump, a flow meter, and a mercury manometer. The microreactor was filled with the loosely packed oxide. The sampling valve enabled us to withdraw small amounts of the circulating gases and to transfer these to the column of a gas chromatograph. The piston pump maintained a gas velocity of $100 \text{ cm}^3 \text{ min}^{-1}$, the total volume of the apparatus being in the order of 200 cm^3 . A helium atmosphere around the exterior of the piston prevented leakage of air into the apparatus.

The apparatus was filled with helium and 1-butene at a constant ratio as regulated by flow meters. After closing the system, the pump was started and a sample was injected into the GLC-column to control the absence of air and the amount of 1-butene present in the apparatus. Then a movable furnace was heated to the reaction temperature desired, subsequently the catalyst was heated rapidly by transferring the hot furnace to its position round the catalyst. During warming up and during reaction the manometer noted pressure increases of 10 to 20 mm mercury. A tube with anhydrous CaCl_2 served as an adsorbent for the water produced.

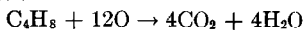
Analysis. The gaseous products were separated by a 6-m column filled with 2,4-dimethylsulfolane on Chromosorb, helium being the carrier gas. Subsequent to the circulation experiments the spent oxide was analyzed by regeneration with oxygen at 773°K . The "coke" which covered the spent oxide was burned off and the amount of carbon dioxide formed was measured by titration. The amount of oxygen taken up by the spent oxide was determined by weighing.

Calculations. The amount of oxygen given off by the catalyst was calculated from the percentages of the various gaseous components assuming following reactions:

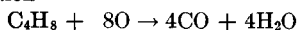
Diene formation



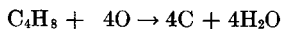
CO₂ formation



CO formation



'Coke' formation



RESULTS

These are divided in three parts:

(I) Experiments at constant temperature and varying time of reduction with Bi₂O₃, MoO₃, and bismuth molybdate, respectively.

(II) Temperature dependency of the rate of reduction of MoO₃ and of bismuth molybdate. Calculation of rate constants and of diffusion coefficients.

(III) Circulation experiments at constant temperature and varying time of reduction with nonstoichiometric molybdenum oxides.

I. Reduction of Bi₂O₃, MoO₃, and Bismuth Molybdate

The results are given as plots of the amounts of oxidation products formed versus circulation times.

A. Reduction of Bi₂O₃

Figure 1 represents the reduction of 200 and of 500 mg of Bi₂O₃ at 793° and 803°K, respectively. The reaction proceeds only slowly and the amount of butadiene is much smaller than that of carbon dioxide. At the beginning the color of Bi₂O₃ changed from orange to gray and at the end of reaction pure Bi metal was found in the spent oxide together with 1.2 mg of coke.

Only traces of isomerization products such as *trans*- and *cis*-2-butenes were observed. The main product is carbon dioxide while carbon monoxide is not observed in the reaction products.

B. Reduction of MoO₃

The results of an experiment in which 200 mg of MoO₃ was reduced at 811°K are represented in Fig. 2. The rate of reaction is much faster than on Bi₂O₃ but it seems to possess an induction period after which the rate accelerates to go through a maximum. The most important products are the 2-butenes. CO₂ and CO are also formed in quantities that are commensurable with butadiene.

The maxima in the CO₂ and CO produc-

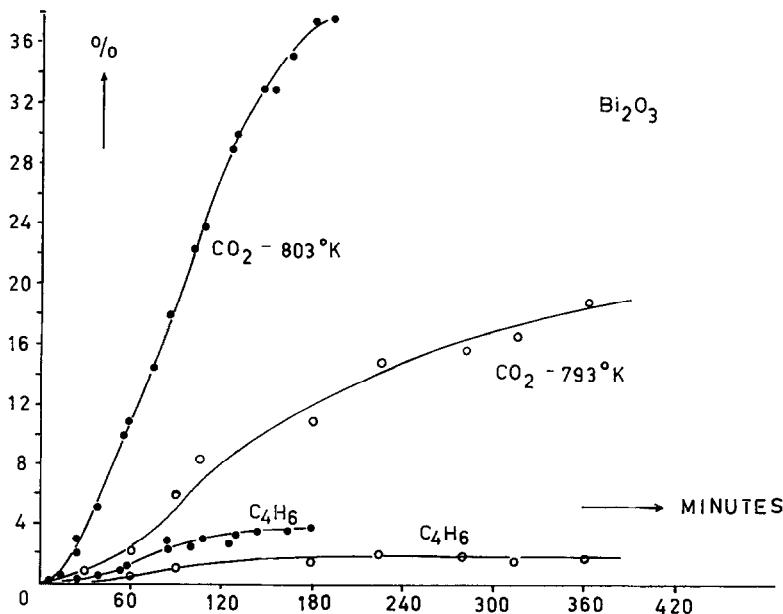


FIG. 1. Reductions of 200 mg and of 500 mg of Bi₂O₃ at 793° and at 803°K started with 40 cm³ and with 41 cm³ 1-butene, respectively.

tions occur at a later time than that of butadiene, which might point to the possibility that they are formed from the diene. In the initial stage of the reaction equal amounts of *cis*- and *trans*-2-butenes are formed, but on further reaction the *cis* isomer begins to predominate.

Reoxidation of the reduced molybdenum oxide was shown to lead to an oxygen up-

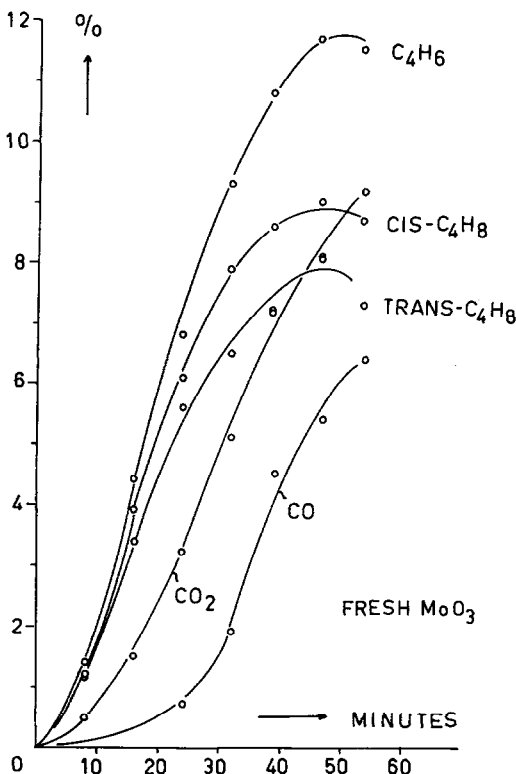


FIG. 2. Reduction of 200 mg of fresh MoO_3 at 811°K started with 46 cm^3 1-butene.

take of 21.6 mg. In addition 1.9 mg of coke was burned off. From the assumptions given in the Experimental Procedure section under "Calculations" (above), we have calculated a total consumption of oxygen of 21.4 mg which is in satisfactory agreement with the value given above. Moreover, it agrees with the reduction of 200 mg of MoO_3 to 178.5 mg of MoO_2 and hence there is some justification for the conclusion that the reduction does not proceed further than to MoO_2 .

The results of an experiment in which 200 mg of precalcined MoO_3 was reduced at

783°K show the overall rate of reaction to be definitely slower than on fresh MoO_3 , but the final conversion to butadiene and the product distribution were similar.

C. Reduction of Bismuth Molybdate

The reduction of 200 mg of bismuth molybdate, catalyst B-48/52, at 783°K is represented in Fig. 3. The overall rate of reaction is much faster than on MoO_3 and there is no induction period. The most important product is butadiene. From the steadily increasing CO and CO_2 productions one might deduce that these products are formed from the diene at a later stage. The *cis/trans* ratio of the 2-butenes was equal to 1 during the whole reaction period. Reoxidation of the reduced bismuth molybdate resulted in a takeup of 15.2 mg of oxygen. In addition 2.1 mg of coke was burned off. A total oxygen consumption of 16.6 mg calculated from the end products formed is in approximate agreement herewith. No separate phase of metallic bismuth was observed in the spent catalyst.

In a preceding paper (1) we reported an inactive bismuth molybdate, viz., catalyst B-50/50. It was deemed useful to check this catalyst also on reducing capacity. The reduction of 200 mg of this catalyst with 1-butene has been carried out at a temperature of 783°K . The CO and CO_2 formations are about equal to those in Fig. 3 but the isomerization and the butadiene formation are far less than those reported above.

II. Temperature Dependency of the Rate of Reduction of MoO_3 and of Bismuth Molybdate

A. Molybdenum Oxide

The analytical results of reoxidation of the reduced molybdenum oxides are given in Table 2 together with the oxygen consumptions calculated from the end products formed after reduction. This table shows that the final consumption of oxygen is independent of temperature of reduction and that the reduction of 200 mg of fresh MoO_3 seems not to proceed further than to Mo^{IV} (21.5 mg oxygen). From the gaseous products formed during the reductions the

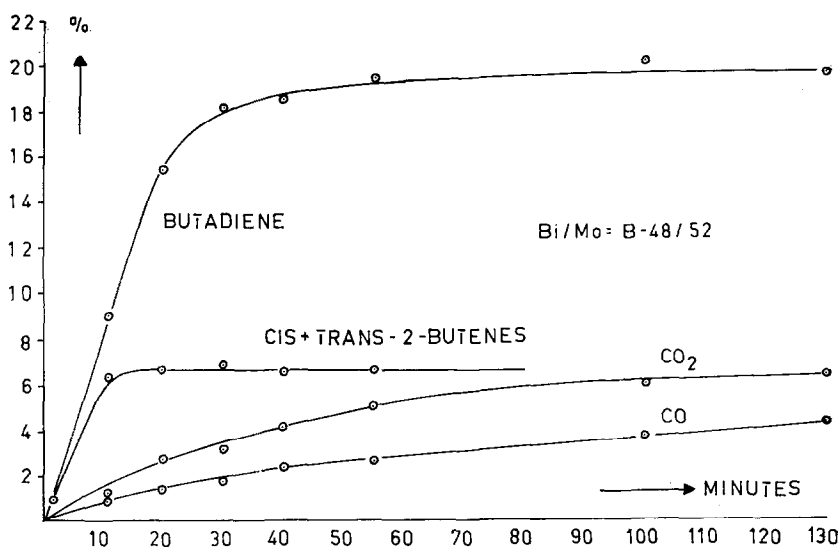


FIG. 3. Reduction of 200 mg of bismuth molybdate (catalyst B-48/52) at 783°K started with 46 cm³ 1-butene.

TABLE 2
COMPARATIVE DATA OF OXYGEN CONSUMPTION AT
DIFFERENT TEMPERATURES OF REDUCTION

Temperature of reduction (°K)	Final oxygen consumption (mg)		Coke formation (mg)
	Analyzed	Calculated	
746°	21.9	20.2	1.7
773°	20.8	18.8	1.1
805°	22.1	20.4	1.2
838°	20.5	20.1	0.9

constants A and B in Eq. (7) are calculated with the least-squares method. They are summarized in Table 3. The "fit" of the

experimental data in the $t^{1/2}$ plot is shown in Fig. 4 and is seen to be remarkably good.

The surface area (S) of the MoO₃ used was 0.35 m² g⁻¹, its density (ρ) was 4.5 g cm⁻³. From these data and from the values of A and B at the temperatures mentioned, the corresponding rate constants (α), diffusion constants (D), and values of $t_0^{1/2}$ are calculated. They are also summarized in Table 3.

B. Bismuth Molybdate

The degree to which 200 mg of bismuth molybdate can be reduced appears to be

TABLE 3
RATE CONSTANTS (α), DIFFUSION COEFFICIENTS (D), AND t_0 OF FRESH MoO₃ AND OF BISMUTH MOLYBDATE

	T (°K)	$10^3 \times B$ (sec ^{-1/2})	$10^3 \times A$ (-)	$10^3 \times \alpha$ (cm sec ⁻¹)	$10^{14} \times D$ (cm ² sec ⁻¹)	$t_0^{1/2} = (1/\alpha)D^{1/2}$ (sec ^{1/2})
MoO ₃ ^a	746	14.7	703	1.55	70	53
	773	20.4	816	2.57	135	45
	805	24.5	503	5.99	193	23
	838	34.3	503	11.80	380	17
Bi/Mo ^b = 48/52	687	4.87	574	2.08	7.7	13
	725	8.58	372	9.96	23.8	4.9
	783	18.10	942	17.51	106	5.9
Bi/Mo ^b = 50/50	783	11.9	311	3.30	95	29.5

^a From Eq. (7).

^b From Eq. (8).

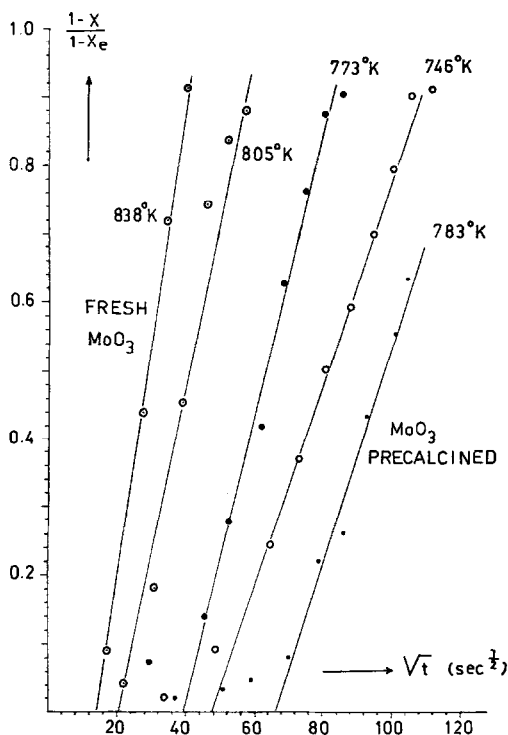


Fig. 4. Equation (7) for fresh MoO_3 at four different temperatures and for precalcined MoO_3 .

strongly dependent on the temperature, as can be observed in Table 4 with comparative data of oxygen consumption at the end of reduction. The highest oxygen consumption

TABLE 4
OXYGEN CONSUMPTION AT DIFFERENT TEMPERATURES

Temperature of reduction (°K)	Final oxygen consumption (mg)		Coke formation (mg)
	Analyzed	Calculated	
687	2.6	3.4	0.8
725	7.4	9.0	1.1
783	15.2	16.6	2.1

observed showed to be nearly equivalent to reduction of Bi^{III} and Mo^{VI} to Bi^{O} and Mo^{IV} .

In the same way as we did for MoO_3 and substituting for S and ρ values of $0.26 \text{ m}^2 \text{ g}^{-1}$ and 6.0 g cm^{-3} , respectively, we calculated α , D , and $t_0^{1/2}$. (See Table 3.) In Fig. 5 the plot of Σ as a function of $(t/t_0)^{1/2}$ is

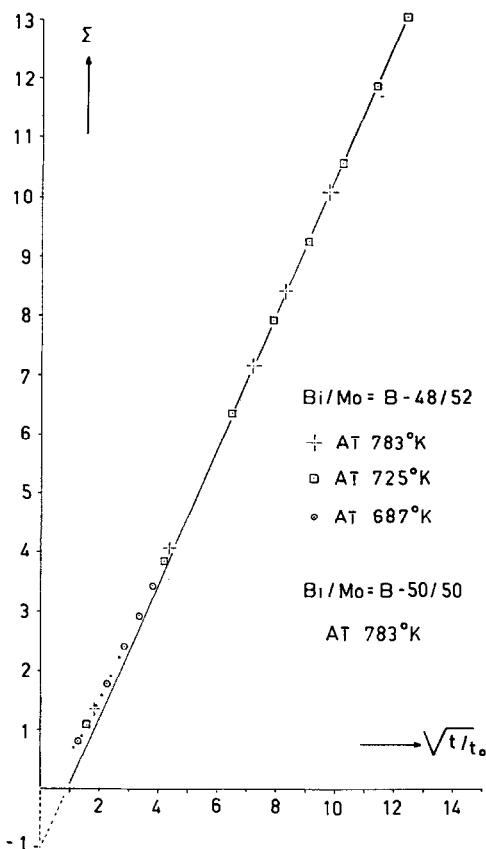


Fig. 5. The mathematical equation (8) for the data of the catalysts B-48/52 and B-50/50.

given. The results with sample B-50/50 with $S = 0.18 \text{ m}^2 \text{ g}^{-1}$ are incorporated in this figure.

III. Circulation Experiments with the Nonstoichiometric Molybdenum Oxides Mo_4O_{11} , $\text{Mo}_{17}\text{O}_{47}$, Mo_8O_{23} , and $\text{Mo}_{18}\text{O}_{52}$

Only the most relevant data, particularly those corresponding to the butadiene formation, are reported here.

The reductions were carried out with 200 mg of the nonstoichiometric compound at a temperature of 793°K . The results are represented in Fig. 6. The diene formations on precalcined MoO_3 at a reaction temperature of 783°K and on fresh MoO_3 at 811°K are incorporated in this figure. It can be seen that all compounds showed induction periods except $\text{Mo}_{17}\text{O}_{47}$. This latter compound was

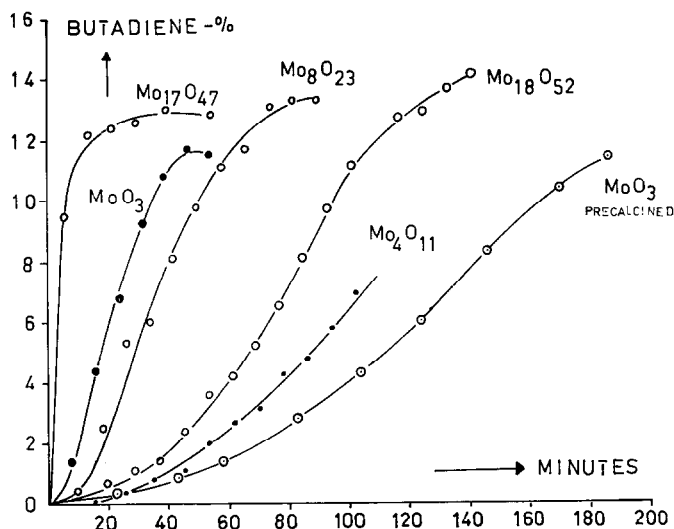


FIG. 6. Butadiene formation during reductions of 200 mg of $\text{Mo}_{17}\text{O}_{47}$, Mo_8O_{23} , $\text{Mo}_{18}\text{O}_{52}$, and Mo_4O_{11} at 793°K started with 45.7, 47.1, 50.0, and 49 cm^3 1-butene, respectively.

already extremely active at the start of reduction.

The results of calculation of the slopes (B) and the intersections (A) in Eq. (6) are summarized in Table 5. The reaction with

TABLE 5
THE SLOPES (B) AND INTERSECTIONS (A) OF EQ. (6) FOR THE NONSTOICHIOMETRIC COMPOUNDS, PRECALCINED MoO_3 , AND Bi_2O_3

Compound	T ($^\circ\text{K}$)	$10^3 \times B$ ($\text{sec}^{-1/2}$)	$10^3 \times A$ (—)
Mo_8O_{23}	793	20.5	492
$\text{Mo}_{18}\text{O}_{52}$	793	22.3	1089
Mo_4O_{11}	793	15.2	778
Precalcined MoO_3	783	15.7	1036
Bi_2O_3	783	9.3	369

$\text{Mo}_{17}\text{O}_{47}$ was so fast that no reliable values could be obtained.

ISOMERIZATION-DEHYDROGENATION

According to the reaction scheme given in the introduction, the ratio (R) of isomerization products and dehydrogenation products is an important quantity to indicate the nature of the catalyst surface sites. In Fig. 7 the ratio ($R = 2\text{-butenes}/\text{butadiene}$) is represented as function of the conversion $[(1 - X)/(1 - X_0)]$ for fresh MoO_3 and for the catalyst B-48/52. It is seen from this

figure that the ratio (R) is high for MoO_3 and dependent on temperature. For the catalyst B-48/52 the ratio is low and almost independent of temperature.

The nonstoichiometric compounds show similar results for the ratio (R) as MoO_3 . Mo_4O_{11} initially shows an R value about equal to that of MoO_3 but this decreases rapidly to about 1.5. $\text{Mo}_{18}\text{O}_{52}$ and Mo_8O_{23} possess R values of about 1.5 and 1.0 that decrease only slightly with the conversion. Finally $\text{Mo}_{17}\text{O}_{47}$ is also exceptional in its isomerization activity in showing R values of 4-3.

DISCUSSION

From the results given before we can make a qualitative comparison between the rate of oxidative dehydrogenation and that of the catalyst reduction.

The $\text{Bi}_2\text{O}_3\text{-MoO}_3$ catalyst is an active catalyst for the oxidative dehydrogenation at temperatures between 400° and 500°C while it is also selective in being only slightly active for double-bond isomerization. In the same temperature range its surface layers are rapidly reduced by 1-butene, the product being mainly butadiene. Relatively inactive species of the catalyst also show a decreased activity for being reduced.

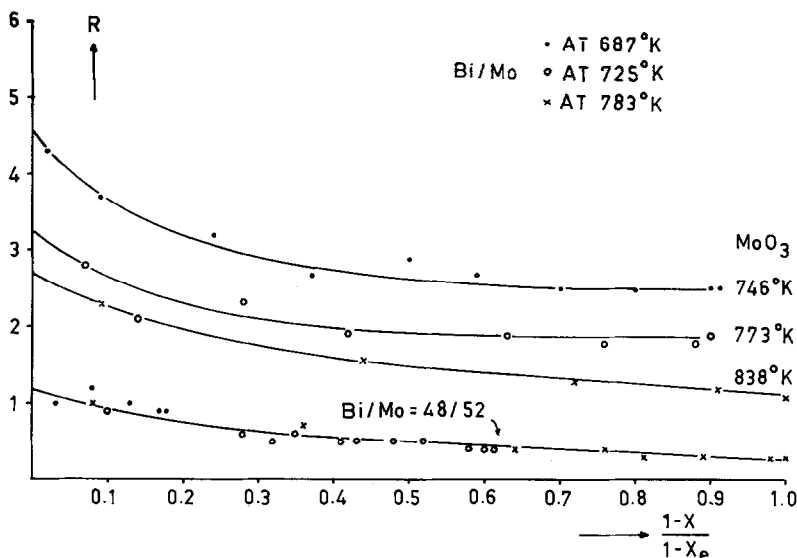


FIG. 7. The isomerization-dehydrogenation ratio as a function of the conversion.

MoO_3 is only slightly active for dehydrogenation in the temperature range mentioned but shows a fairly good isomerization activity. Its initial rate of reduction is also slow and becomes appreciable only after some reduction has occurred. Among the products we observe that the 2-butenes are present in considerable excess in satisfactory agreement with the catalytic activity of this compound.

Qualitatively there is hence a strong resemblance between the rate of the oxidative dehydrogenation and the rate of reduction, thus leading to the impression that the rate-determining reaction in the catalysis is identical with the surface reduction of the catalyst. We may now attempt to put this qualitative similarity on a somewhat firmer quantitative basis. As has been said before one then has to extrapolate reduction measurements that actually refer to compounds in an advanced state of reduction to situations that involve only a minor oxygen depletion, i.e., one should reconstitute the surface reaction from experiments in which a considerable part of the underlying solid is already reduced and in which the reduction is mainly determined by diffusion of oxygen ions in the solid.

A clear understanding of the diffusional mechanism is therefore necessary before an

attempt to unravel the mechanism of the surface reaction can be made.

A. The Diffusion Constant

The reduction experiments furnish two sets of data from which numerical values for the diffusion constants can be obtained:

- (1) the reduction of $\text{Bi}_2\text{O}_3\text{-MoO}_3$ catalysts that can be represented mathematically by either Eq. (7) or (8) and with t_0 values of 10–100 sec.
- (2) the reduction of MoO_3 samples that fit Eq. (7) with relatively high t_0 values (500–2500 sec) but that do not fit Eq. (8).

From the slope (B) of Eq. (7) values for D can be obtained if S and ρ are known. However, the D values for MoO_3 are somewhat suspect in view of the deviations from the expected kinetics.

It is therefore of interest in this connection that von Destinon-Forstmann (8) published experimental results on the reduction of MoO_3 by hydrogen. The mathematical model applied there to explain the results differs from that used by us. On inspection, however, it is found that these results are equally well represented by Eqs. (7) and (8) with t_0 values of the order 100–500 sec (see Table 6). Evidently the reduction by hydrogen involves a different surface reaction but the

TABLE 6
THE DIFFUSION CONSTANTS (D) AND RATE
CONSTANTS (α) FOR THE REDUCTION OF MoO_3
BY HYDROGEN CALCULATED FROM THE SLOPES
(B) AND INTERSECTIONS (A) OF EQ. (7) FROM
EXPERIMENTAL DATA OF VON
DESTINON-FORSTMANN^a

T (°K)	$10^3 \times B$ ($\text{sec}^{-1/2}$)	$10^3 \times A$ (—)	$10^3 \times \alpha$ (cm sec^{-1})	$10^{14} \times D$ ($\text{cm}^2 \text{sec}^{-1}$)	$t^{1/2} =$ ($1/\alpha$) $D^{1/2}$ ($\text{sec}^{1/2}$)
673	5.3	106	1.52	11.9	22.7
723	10.3	215	2.89	46.0	23.5
773	13.4	132	7.95	77.7	11.1
823	23.2	164	19.09	231.9	8.0

^a Assumed was $S = 0.30 \times 10^4 \text{ cm}^2 \text{ g}^{-1}$ and $\rho = 4.5 \text{ g cm}^{-3}$.

numerical values of the diffusion constant obtained in the two sets of experiments should be the same.

Figure 8 shows the various values of D

obtained at different temperatures in the form of a $\log D$ versus $1000/T$ plot. The data obtained from the hydrogen reduction were calculated assuming S and ρ of the von Destinon-Forstmann samples to be identical to those of our samples. It is seen that the two sets of D values for MoO_3 are very similar and can be considered to be equal within the accuracy of the experiments. Therefore the interpretation given to the B parameter of Eq. (7) also seems to hold for the reduction of MoO_3 by 1-butene. In the temperature range around 800°K the D values for MoO_3 and $\text{Bi}_2\text{O}_3\text{-MoO}_3$ appear to be equal although there is some indication that at lower temperatures the diffusion in bismuth molybdate is more difficult.

The straight lines in Fig. 8 are connected to the relation

$$D = D_0 \exp(-E_D/RT) \quad (16)$$

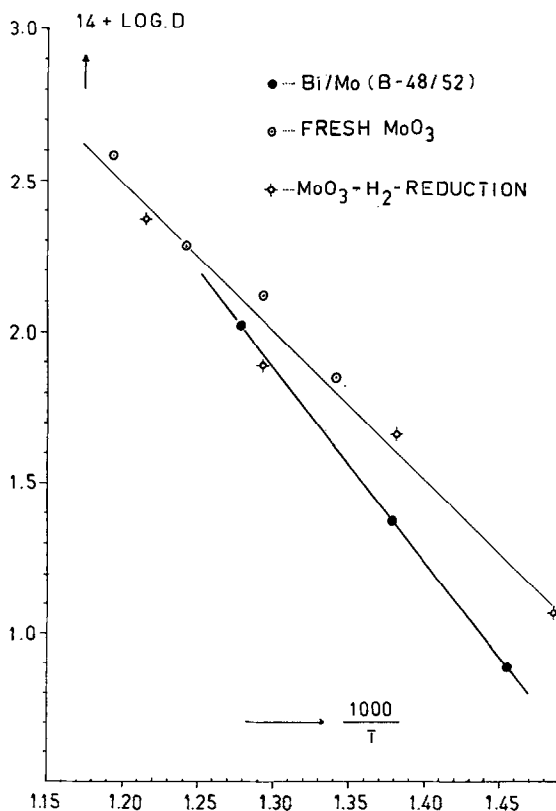


FIG. 8. The diffusion constant dependency on temperature for the catalyst B-48/52, for fresh MoO_3 , and for MoO_3 prepared by von Destinon-Forstmann.

The parameters for the different samples are as follows:

$$\text{Bi/Mo} = 48/52$$

$$\log D_0 = -3.73 \quad E_D = 29.3 \text{ kcal mole}^{-1}$$

MoO₃ (butene reduction)

$$\log D_0 = -5.62 \quad E_D = 22.1 \text{ kcal mole}^{-1}$$

MoO₃ (H₂ reduction)

$$\log D_0 = -6.145 \quad E_D = 20.6 \text{ kcal mole}^{-1}$$

MoO₃ combined values

$$\log D_0 = -5.686 \quad E_D = 22.0 \text{ kcal mole}^{-1}$$

According to the absolute rate theory (Glasstone, Laidler, Eyring)

$$D_0 = (\lambda^2 kT/h) \{1 - \exp(-h\mu/kT)\} \quad (17)$$

where λ is the jump distance and ν the frequency of the vibration of the migrating species in its rest position. Taking λ to be 3×10^{-8} cm, the term $\lambda^2 kT/h$ is of the order 10^{-2} , which is near enough to the experimental values, in view of the fact that $h\mu$ should be of the order of kT . The experimental D values obtained by us are therefore of the correct order of magnitude.

The observation that D is equal for Bi₂O₃-MoO₃ and MoO₃ at temperatures around 800°K might be extrapolated to other MoO₃-containing compounds such as the nonstoichiometric Mo oxides. Since for most of these $S\rho$ is not known, this quantity could now be obtained from the B parameter assuming D to be equal to D of MoO₃ or of bismuth molybdate. The knowledge then of $S\rho$ should enable us to calculate α which

is the parameter in which we are primarily interested. Values obtained in this manner are assembled in Table 7.

B. The Reaction at the Surface

Figure 9 and Table 7 contain a summary of the experimental values of α obtained from Eq. (7). For the reduction of bismuth molybdate by 1-butene and of MoO₃ by hydrogen these values can be interpreted in accordance with the boundary condition (2). Their interpretation for the reduction of MoO₃ and the nonstoichiometric Mo oxides remains somewhat less obvious. The $\log \alpha$ versus $1/T$ plot for the bismuth molybdate reduction is seen to be curved in good agreement with the results found for the oxidative dehydrogenation of 1-butene over this catalyst [see ref. (1)]. It can, moreover, be shown that the rate of reduction and the rate of oxidation are approximately equal for bismuth molybdate; this is calculated now for a temperature of 460°C.

The $\log \alpha$ value at this temperature is equal to -6.9 . Using a λ value of 3×10^{-8} cm (the diameter of an O²⁻ ion) we find from the relationship $\alpha = \lambda k_s$ that $k_s \simeq 4 \text{ sec}^{-1}$; half the available oxygen from the surface is therefore converted in 1/4 sec. For 1 g of catalyst (with an apparent volume of 1/2 cm³ and a surface area of $3 \times 10^8 \text{ cm}^2$) the total number of surface O²⁻ ions (surface area 9 Å²) is 3×10^{18} . Of these about half can be removed, i.e., 1.5×10^{18} . In 1 sec therefore 6×10^{18} oxygen ions react with 1-butene to give 6×10^{18} molecules of

TABLE 7
COMPARISON OF RATES OF SURFACE REACTIONS FOR MO-CONTAINING COMPOUNDS AT 783°K
AND AT 793°K^{a,b}

Sample	$10 \times A$ (-)	$10^2 \times B$ (sec ^{-1/2})	S (m ² × g ⁻¹)	$10^8 \times \alpha$ (cm sec ⁻¹)	$10^{14} \times D$ (cm ² × sec ⁻¹)	$R_0 \rightarrow R_\infty$
Bi/Mo = 48/52 783°K	9.42	18.10	0.26	17.5	106	1 0.5
Bi/Mo = 50/50 783°K	3.11	11.87	0.18	3.3	95	0.1 0.3
MoO ₃ fresh 783°K			0.35	2.8	145	3 2
MoO ₃ precalc. 783°K	10.36	15.67	(0.26)	1.6	145**	3 2
Mo ₄ O ₁₁ 793°K	7.78	15.19	(0.24)	2.2	157**	2.7 1.6
Mo ₆ O ₂₃ 793°K	4.92	20.52	(0.33)	4.6	157**	1.2 0.8
Mo ₁₅ O ₅₂ 793°K	10.89	22.27	(0.35)	2.3	157**	1.6 1.1

^a Density of the nonstoichiometric Mo oxides assumed to be 4.5 g cm⁻³.

^b Numbers marked with ** are assumed; numbers in parentheses are calculated values herefrom.

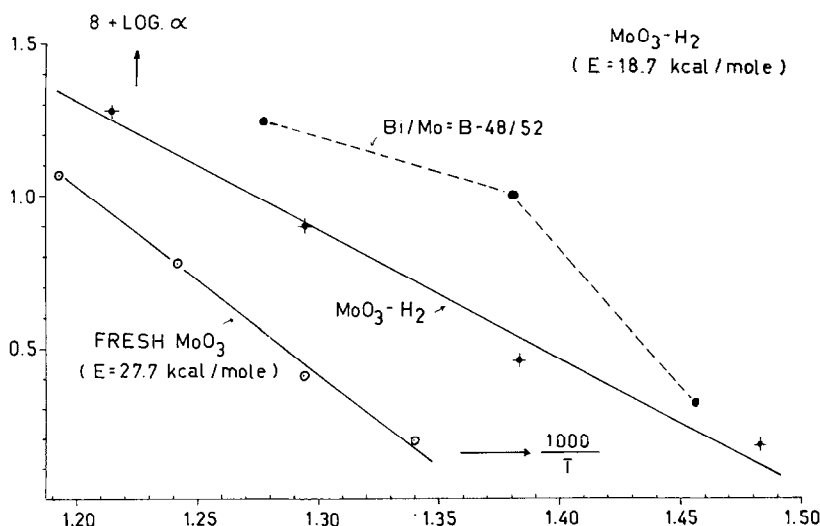


FIG. 9. The rate constant dependency on temperature, for fresh MoO_3 , and catalyst B-48/52 in reaction with 1-butene and for MoO_3 in reaction with hydrogen.

butadiene ($1/4 \text{ cm}^3$). So per cm^3 of catalyst, 0.5 cm^3 of butadiene is formed per second.

For the catalytic experiment at GHSV = 4200, i.e., about one volume butene per volume catalyst, a conversion of 63% is observed, which means that per cm^3 of catalyst, 0.63 cm^3 of butadiene is formed per second. Within the accuracy of our experiments and the uncertainty in the factors involved in the calculations the two rates appear equal.

Our conclusion is therefore that in view of the close qualitative and quantitative correspondence between reduction and oxidative dehydrogenation for bismuth molybdate, the latter reaction starts as a reduction of the catalyst, in good agreement with the theory proposed.

The smaller activity of the MoO_3 samples is reflected in the considerably smaller values for α . To explain a small α one might consider the following possibilities:

- α is smaller because k'' in a boundary condition such as given by Eq. (2) is small;
- it is smaller because the subsequent dehydration is slow;
- it is smaller because it is connected with a boundary condition of the type (9) with the additional condition that (1

— θ_s), i.e., the vacancy concentration, is small.

Assumption (b) cannot be valid since the reduction by hydrogen that also involves a dehydration step possesses a relatively large α value. Assumption (a) suffers from the inability to explain the existence of an induction period. Therefore assumption (c) appears to be the most likely cause. It then remains to explain why MoO_3 contains so few vacancies on its surface.

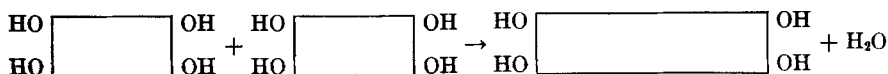
The structure of MoO_3 is represented in Fig. 10. It consists of double layers that in the plane of the layers are given by Fig. 10a and perpendicular to this plane by 10b. The layers therefore are constituted by having O^{2-} layers on the outside except at the edges. Here, there are either OH^- ions (see 10c and d) or alternatively pairs of O^{2-} + vacancy sites obtained by dissociation of H_2O from a pair of OH^- groups. The layers are stacked on top of each other so that the outer surface consists of planes with O^{2-} ions or with hydroxyl, respectively, O^{2-} vacancy pairs.

Since the MoO_3 samples usually consist of platelike crystals, the greater part of the outer surface may be considered to be formed by O^{2-} ions, thus explaining the relatively

small concentration of vacancies at the outer surface. Reduction there may be supposed to begin at the edges and therefore to be slow in the initial stages of the reaction. Because of migration of O^{2-} ions from the layer planes to the edges, the former will gradually acquire a certain concentration of vacancies with a consequent increase in the rate of reduction. In the catalytic reaction, however, these vacancies will be filled by oxygen from the gas phase so that only the edges remain active.

Hence, our final conclusion: *MoO₃ sites active for the catalysis are mainly located on the edges of the layers, a situation highly reminiscent of that postulated by Arlman (9) for the Ziegler-Natta polymerization over TiCl₃.*

Precalcination of MoO₃ might be considered to lead to an increase in the number of layers stacked on each other, a process that should cause a considerable decrease of surface area. It might also entail a growth of the layer dimension in one direction by the fusing of edges, such as



The latter reaction would not lead to a substantial decrease in surface area but it would decrease the number of active sites and therefore increase the initial period of increase of speed of reduction.

From Table 7 we see that *S* does not decrease very much as shown by the relative constancy of the *B* factor in Eq. (7) but α decreases more strongly, in satisfactory agreement with the second model of crystal growth discussed.

C. The Relative Rate of Isomerization and Dehydrogenation

Table 7 summarizes the selectivities for a number of Mo-containing compounds as given by the ratio $R = 2\text{-butenes formed/butadiene formed}$. The *R* values in this table refer to the selectivity in the initial stages of the reduction (R_0) and at almost complete reduction (R_∞). It is seen that the R_∞ values are generally lower than the R_0 values, i.e., the surface reaction becomes more selective

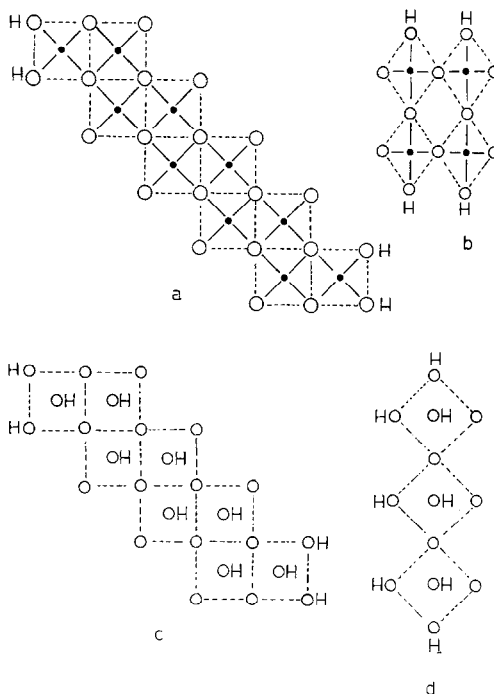
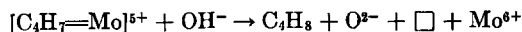


FIG. 10. The structure of MoO₃.

for oxides that are considerably reduced. Let us first consider the R_0 values. They are seen to vary considerably for the different oxides, and it is to be noted that the differences between bismuth molybdate and MoO₃ are again closely similar to those observed in the catalytic reaction. Another question is whether we can understand the differences in selectivity. We have postulated the isomerization reaction to be the reverse reaction of (1), i.e.,



and the formation of butadiene as



Therefore *R* must depend on the relative concentration of OH^- and O^{2-} in the direct vicinity of the site. Let us suppose that every vacancy has z neighbor anions and that a fraction θ_{OH} is originally present as OH^- . After formation of the allyl complex there will be $(\theta_{\text{OH}}z + 1) \text{OH}^-$

ions and $\{(1 - \theta_{\text{OH}})z - 1\} \text{O}^{2-}$ ions. Therefore

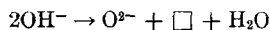
$$R = \gamma \frac{0.5(\theta_{\text{OH}} + 1/z)}{(1 - \theta_{\text{OH}}) - 1/z} \quad (18)$$

where γ is an *a priori* probability and the factor 0.5 in the denominator accounts for the possibility that the formation of butene can lead both to 1-butene and 2-butene which are assumed here to be equally probable. We shall further suppose in the following that γ is equal for all compounds investigated. Now, for the catalyst B-50/50 we find an extremely low R (≈ 0.1). Putting $\theta_{\text{OH}} = 0$ and $z = 4$ we find that γ is of the order of 1.

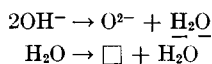
Therefore, as an approximation we write

$$R \approx \frac{0.5(\theta_{\text{OH}} + 1/z)}{(1 - \theta_{\text{OH}}) - 1/z}$$

The two parameters that define R are therefore θ_{OH} and z . A high θ_{OH} assumes the reaction



to be slow. The mechanism of the dehydroxylation must be as follows:



where $\underline{\text{H}_2\text{O}}$ means a surface-bonded water molecule.

Now, the heats of hydration of H_2O on metal cations increase strongly with the charge of the cation. Therefore Bi^{3+} (H_2O) should dissociate its water ligand faster than Mo^{6+} and even Mo^{4+} . We believe this effect to be of prime importance in determining the low θ_{OH} and therefore the greater selectivity of the bismuth molybdate.

However, even for slow dehydroxylation, where θ_{OH} is high, the concentration of OH^- cannot be appreciable unless it is assumed that the site density is high. The H atoms are deposited on the surface by the dehydrogenation but the particular site on which this occurs becomes temporarily deactivated. For active sites to be surrounded by OH we have to assume the presence of deactivated sites in their immediate neighborhood, which points to a large concentration of sites. For

R to be low, the number of neighbor anions z should be high. If, for instance, $z = 2$ the statistical probability that an allyl complex can donate an H atom to an oxygen ion becomes low because already one of the surrounding anions has accepted an H atom.

These two factors, high density of sites and low z , seems to fit the MoO_3 structure in a remarkably good manner. Looking again at Fig. 10 we see that the configurations, supposed to be active, are located on the edges (10c and d). On one edge type there occur isolated groups of two anion sites, on the other a zigzag row of such sites. At best therefore $z = 2$. The model given above, which accounts for the increase in reducibility, is therefore also in agreement with the relative importance of the isomerization reaction.

D. The Activity and Reducibility of the Nonstoichiometric Mo Oxides

The nonstoichiometric Mo oxides, apart from $\text{Mo}_{17}\text{O}_{47}$, are similar in their reactivity pattern to MoO_3 . Generally speaking, however, their R_0 values are lower than for MoO_3 . This might perhaps be explained from the fact that their structures are derived from the ReO_3 structure, i.e., a structure that does not present the localization of sites on special crystal faces and therefore does not show the high surface density of sites nor the low z value characteristic for the double-layer MoO_3 lattice. $\text{Mo}_{17}\text{O}_{47}$ presents an interesting deviation of the generally observed reaction patterns. It reacts very rapidly with 1-butene under copious formation of 2-butenes and without an induction period being present. Since it is formed by interaction of MoO_2 and MoO_3 at temperatures around 500°C one might consider the possibility that it is formed during the reduction of MoO_3 , thereby explaining the increase in rate of reduction in the initial stages of the reaction. Actually, of course, this involves an increase of D , the diffusion constant, with increasing oxygen depletion. However, it is difficult to envisage why reduction by hydrogen that is fast from the very beginning of the reaction does not profit from the possible formation of this intermediate compound.

We therefore believe that it is not formed during either the reduction by 1-butene or hydrogen. Why then is it so active? This may have to do with its peculiar structure. According to Kihlberg (10) it consists of a complicated pattern obtained by connecting polyhedra, some octahedra but also pentagonal bipyramids, sharing corners and edges. The structure contains "tunnels" that normally are blocked by "dangling" oxygen ions. Reduction, however, may remove precisely these blocking ions so that the surface area increases with increasing reduction, thus explaining the fast rate of reduction. Why it is such an active isomerization catalyst remains unexplained, however.

REFERENCES

1. BATIST, PH. A., LIPPENS, B. C., AND SCHUIT, G. C. A., *J. Catalysis* **5**, 55 (1966).
2. ADAMS, C. R., *Proc. Intern. Congr. Catalysis, 3rd, Amsterdam, 1964* **1**, 240 (1965).
3. SACHTLER, W. H. M., AND DE BOER, N. H., *Proc. Intern. Congr. Catalysis, 3rd, Amsterdam, 1964* **1**, 252 (1965).
4. CRANK, J., "The Mathematics of Diffusion," p. 34. Oxford, Clarendon, 1957.
5. HAUL, R., JUST, D., AND DÜMBGEN, G., Sauerstoff Diffusion in Oxyden. *Proc. Intern. Symp. Reactivity of Solids, 4th, Amsterdam, 1960*. (Elsevier, 1961).
6. HAUL, R., DÜMBGEN, G., AND JUST, D., *Z. Physik. Chem. (Frankfurt)* **31**, 309 (1962).
7. MAGNÉLI, A., *Acta Chem. Scand.* **2**, 501 (1948); **2**, 861 (1948); KIHLBORG, L., *ibid.* **13**, 954 (1959); KIHLBORG, L., *Arkiv Kemi* **21**, 443, 461 (1963).
8. VON DESTINON-FORSTMANN, J., *Can. Metallurg. Quart.* **4**, 1 (1965).
9. ARLMAN, E. J., *J. Catalysis* **3**, 89 (1964).
10. KIHLBORG, L., "The Crystal Chemistry of Mo Oxides." *Advan. Chem. Ser.* **39**.